Ab Initio Molecular Dynamics Study of Metallocene-Catalyzed Ethylene Polymerization

Robert J. Meier,*,† Gerard H. J. van Doremaele,† Simonetta Iarlori,‡ and Francesco Buda‡

Contribution from DSM Research, P.O. Box 18, 6160 MD Geleen, The Netherlands, and IBM European Centre for Scientific and Engineering Computing, Viale O. Pacifico 171, I-00144 Rome, Italy

Received February 11, 1994. Revised Manuscript Received May 4, 1994•

Abstract: This is the first report on the simulation of the full dynamics, at a quantum mechanical level, of a catalytic chemical reaction. Ab initio molecular dynamics simulations on ethylene insertion in a bridged dicyclopentadienylmethylzirconocene have revealed that the entire reaction path starting from the π-coordinated ethylene–zirconocene complex up to and including propyl formation takes place in about 150 fs, which is unexpectedly fast. This observation suggests the absence of any significant barrier of activation, as confirmed by static energy minimizations. The Cp rings are very flexible. Starting from a reactant structure without α-agostic interaction, at $T = 400$ K such an interaction evolves during the course of the insertion reaction and before the propyl is formed. The product state exhibits γ-H agostic interaction.

1. Introduction

One of the most important industrial polymerization reactions concerns the synthesis of polyolefins, classically carried out using Ziegler–Natta-type catalysts. Recently, a new class of catalysts for olefin polymerization, i.e., metallocenes, originating from the pioneering work by Kaminsky et al.,[1] have become the focus of considerable research efforts. The interest in this new type of catalysts is particularly driven by some specific characteristics. First, the metallocenes in their catalytically active form are well-defined species and (almost) every individual complex is active, in contrast with the classical Ti- and V-based Ziegler–Natta catalysts, where only 1–5% of the metal sites is active. Second, by modifying the ligand system of the metallocenes it is possible to tailor the polymer structure, e.g., to control polymer chain tacticity. This way metallocenes have the potential to be used for the synthesis of novel types of polyolefins, e.g., syndiotactic polypropylene.

Because the metallocene species are well-defined, they can be well subjected to theoretical calculations at the atomic scale. In fact, starting with the model study by Lauher and Hoffmann,[2] quite a number of model calculations on metallocenes using a variety of approaches have been reported, i.e., employing nonbonded potential energies,[3-9] the extended Hückel theory (EHT)-based method,[10-13] ab initio Hartree–Fock techniques,[3,8,13-15] and ab initio density functional methods.[16,17] We will now briefly summarize previous literature.

Guerra and co-workers[4-7,9] have published a series of papers dealing with the stereochemistry and regiospecificity of α-olefin polymerization, more specifically propylene polymerization. Only the nonbonded potential energies were calculated. The major drawback of this method is that only steric effects are taken into account and no electronic effects, and also the geometry of the set of ligands is not fully energy minimized (fixed bond lengths and bond angles). However, Guerra et al. claim that they have obtained a reasonably good description and understanding on tacticity control during α-olefin polymerization by using this method.

Castonguay and Rappé[8] also studied the stereotacticity for the propylene polymerization, employing a combination of ab initio Hartree–Fock calculations for geometry optimization. An empirical force field approach with the Cp rings replaced by pseudoatoms was used to determine the steric influence of the ligand. The ab initio calculations were restricted to the reaction $Cl_2ZrCH_3^+ + C_2H_4 \rightarrow Cl_2ZrC_3H_7^+$, whereas the force field calculations additionally covered indenyl ligand-containing complexes. Drawbacks in this approach are the lack of accounting for electronic effects and fixing the distance between the Zr atom and its neighboring atoms in the force field calculations and the relatively small mixed basis set in the single ab initio run.

Jolly and Marynick[14] studied the insertion reaction of ethylene into the Ti–C bond of $Cl_2TiCH_3^+$ and $Cp_2TiCH_3^+$. Geometries were optimized at the semiempirical PRDDO level while C_s symmetry was imposed and all C–C and C–H distances in the Cp rings were fixed. Energies were reevaluated at the ab initio Hartree–Fock level employing a mix of 4-31G and STO-3G basis sets, whereas the metal atom was described by a mix of single-ζ up to double-ζ bases. Electron correlation effects were accounted for by performing MP2 calculations.

Brintzinger et al.[10] investigated the olefin insertion in an alkylzirconocene cation, viz. $Cp_2ZrCH_3^+$, applying the extended

* Author to whom correspondence should be addressed.
† DSM Research.
‡ IBM European Centre for Scientific and Engineering Computing.
• Abstract published in *Advance ACS Abstracts*, July 1, 1994.

(1) Anderson, A.; Cordes, H. G.; Herwig, J.; Kaminsky, W.; Merk, A.; Mottweiler, R.; Sinn, J. H.; Vollmer, H.-J. *Angew. Chem., Int. Ed. Engl.* **1976**, *15*, 630.
(2) Lauher, J.; Hoffmann, R. *J. Am. Chem. Soc.* **1976**, *98*, 1729–1742.
(3) Kawamura-Kuribayashi, H.; Koga, N.; Morokuma, K. *J. Am. Chem. Soc.* **1992**, *114*, 8687–8694.
(4) Cavallo, L.; Corradini, P.; Guerra, G.; Vacatello, M. *Polymer* **1991**, *32*, 1329–1335.
(5) Cavallo, L.; Guerra, G.; Vacatello, M.; Corradini, P. *Macromolecules* **1991**, *24*, 1784–1790.
(6) Venditto, V.; Guerra, G.; Corradini, P.; Fusco, R. *Polymer* **1990**, *31*, 530–537.
(7) Corradini, P.; Guerra, G. *Prog. Polym. Sci.* **1991**, *16*, 239–257.
(8) Castonguay, L. A.; Rappé, A. K. *J. Am. Chem. Soc.* **1992**, *114*, 5832–5842.
(9) Cavallo, J.; Guerra, G.; Oliva, L.; Vacatello, M.; Corradini, P. *Polym. Commun.* **1989**, *30*, 16–19.
(10) Prosenc, M. H.; Janiak, C.; Brintzinger, H. H. *Organometallics* **1992**, *11*, 4036–4041.
(11) Janiak, C. *J. Organomet. Chem.* **1993**, *452*, 63–73.
(12) Mohr, R.; Berke, H.; Erker, G. *Helv. Chim. Acta* **1993**, *76*, 1389–1409.
(13) Gleiter, R.; Hyla-Kryspin, I.; Niu, S.; Erker, G. *Organometallics* **1993**, *12*, 3828–3836.
(14) Jolly, C.; Marynick, D. *J. Am. Chem. Soc.* **1989**, *111*, 7968–7974.
(15) Siegbahn, P. E. M. *Chem. Phys. Lett.* **1993**, *205*, 290–300.
(16) Weiss, H.; Ehrig, M.; Ahlrichs, R. *J. Am. Chem. Soc.*, in press.
(17) Woo, T. K.; Fan, L.; Ziegler, T. 40 Years of Ziegler Catalysts: *Book of Abstracts Freiburg Symposium* **1993**, *Sept.*

0002-7863/94/1516-7274$04.50/0

Hückel method. The final species is the *n*-propyl complex $[Cp_2ZrC_3H_7]^+$. Two different reaction modes were analyzed concerning the position of the protons of the ethylene relative to the position of the methyl protons, i.e., a staggered reaction mode and an eclipsed reaction mode. The latter appeared to be the most probable mode on the basis of an energy comparison. It was found that one of the α-H atoms of the migrating methyl group stabilizes the transition state of the preferred reaction mode. Furthermore, it was found that first the alkyl tilts away from the Zr–C bond axis, followed by a olefin shift toward the methyl group. The final species is stabilized by agostic interactions of the γ-H with the Zr atom. The major drawback of this method is the fact that the conventional EHT method does not allow for optimization of the geometry. Thus by starting from related crystal structures, the minimum energy structure has to be found by varying the input geometry "by hand". Necessarily, in order to reduce the number of different geometry possibilities, several symmetry constraints are applied, e.g., both Cp rings have equal $Zr–C_{ring}$ distances. Also, the geometry of the Cp-containing ligand framework was kept constant during olefin insertion.

Janiak[11] also employed the EHT method. This approach did not allow for energy minimization of the structures. The cationic species $Cp_2ZrCH_3^+H_2C{=}CH_2$ was studied. The analysis particularly involved the use of Walsh diagrams. It was concluded that α-agostic interaction plays no role in the reactant species but becomes important along the reaction coordinate.

Morokuma et al.[3] applied ab initio Hartree–Fock calculations to study the insertion of ethylene and a force field method to study the stereocontrol of α-olefin polymerization using the bridged metallocene species $H_2Si(CpR)_2ZrMe^+$. In the ab initio calculations, some symmetry constraints were imposed on the structure. The energetics of the reactant complex, the π-complex, the transition state, and the product of the ethylene insertion into the Zr–C bond were calculated. The product showed a strong β-H agostic interaction. Based on the calculated structure of the transition state, molecular mechanical calculations were carried out to determine the effects of substituents on the Cp rings. By the force field route only the steric effects of the substituents are taken into account.

Siegbahn[15] recently reported high-level ab initio calculations on the relatively simple model species $ZrCH_3^+/H_2C{=}C_2$ and $ZrH_2CH_3^+/H_2C{=}C_2$. However, such simple systems can hardly be seen as realistic models for metallocene catalysts.

Ziegler[17] et al. reported on ab initio density functional calculations in the energy profile for the insertion reaction $Cp_2MCH_3^+ + H_2C{=}CH_2 \rightarrow Cp_2MCH_2CH_2CH_3^+$. The calculations revealed that no π-ethylene complex is involved as an intermediate in the insertion complex. The barrier to insertion amounts to less than 5 kcal/mol. The formed propyl complex can adopt several conformations, including structures in which a C–H bond is involved in β-H or γ-H agostic interactions with the metal center, with the structure with a β-H agostic interaction being the more stable complex. The β-H agostic interaction is particularly stable for M = Zr. This study did not support the view that α-H agostic interactions are important for the stability of the reactant complex or that this would be of any importance during the reaction. However, with regard to this study, very few details are available at present.[17]

Ahlrichs et al.[16] very recently reported calculations on $Cp_2TiCH_3^+H_2C{=}CH_2$ and $Cl_2TiCH_3^+H_2C{=}CH_2$. Electron correlation was accounted for either by MP2 calculations in conjunction with the Hartree–Fock method or by employing the local density functional (LDF) method. No geometrical constraints were imposed during energy minimizations. These calculations and those reported by Ziegler are the only calculations reported so far which have been carried out on species resembling a real catalytic species *and* which are simultaneously carried out at a high (ab initio) level of computation. The results on $Cp_2TiCH_3^+H_2C{=}CH_2$ strongly supported the mechanism proposed by Brookhart and Green,[18] i.e., agostic interactions were found to be crucial. On the other hand, no evidence was found for the Cossee mechanism,[19] i.e., in particular, no "stable" transition state was found at the highest level of calculation. The conclusion drawn herefrom is that the insertion of the ethylene is a spontaneous process. This result was revealed both from the energy minimizations carried out at the Hartree–Fock level including MP2 and from the LDF calculations. A different result was obtained, however, when within the Hartree–Fock method the energy was not minimized at the MP2 level, i.e., an MP2 calculation was carried out on a pure Hartree–Fock optimized structure. For the latter case, a barrier of activation was found to be present, as with a more often employed model system, $Cl_2TiCH_3^+H_2C{=}CH_2$, which, albeit still quite similar to the $Cp_2TiCH_3^+H_2C{=}CH_2$, revealed a barrier of activation at the MP2 level. Ahlrichs et al. concluded that the chlorine derivative is not a suitable model system. In essence, the results presented by Ahlrichs et al. provide evidence that a lot of the aforequoted ab initio work is invalidated, either because of an insufficient basis or because no proper model systems were used. In conclusion, previous results should be treated with care, and any positive agreement with experimental data might be considered fortituous.

In the present paper we present results obtained from ab initio molecular dynamics simulations (Car–Parrinello method[20]) of the insertion of ethylene in an alkylzirconocene cation. This type of simulation has the advantage over conventional energy minimization techniques in that entropy is taken into account implicitly. This implies that one effectively probes free energy space rather than only the enthalpy. In practice, stability of a molecular system and thus also chemical reactions are driven by changes in free energy. For this purpose the ab initio molecular dynamics method seems very suitable.

For comparitive reasons we selected a molecular species studied before with the aid of ab initio techniques. When we started out studies, the aforementioned papers by Ziegler and Ahlrichs had not yet appeared, and we chose the ethylene insertion reaction explicitly studied by Morokuma, viz. ref 3, involving the species $(SiH_2Cp_2)ZrCH_3^+H_2C{=}CH_2$. In fact, because the work of Morokuma et al. was the highest in quality as far as a zirconocene complex is concerned, we took their structures as starting structures for our simulations.

2. Calculational Details

All calculation were run on an IBM RISC 6000 workstation Model 560 with 256 MB RAM memory. The software package employed to carry out the Car–Parrinello method-type calculations is the AIMD package, i.e., *Ab-initio Molecular Dynamics*, which has been developed within IBM/ECSEC and IBM Zürich Laboratories. The Car–Parrinello method[20] combines the molecular dynamics simulation with an accurate description of the interatomic potential which is based on electronic structure calculation. The quantum description of the electronic structure is based on the density functional theory (DFT). The exchange correlation energy functional in the DFT is treated within the local density approximation (LDA). We employ the Perdew–Zunger parametrization for the exchange correlation potential in the homogeneous electron gas.[21]

The molecules treated had dimensions of approximately 6 Å and were placed in a cubic box with a length of 11 Å. Periodic boundary conditions were imposed. The choice of the box size was made to minimize the interaction of the molecule with the neighboring images. We have explicitly checked this point by repeating some calculations with an enlarged box of 13 Å length (this calculation required 320 MB RAM memory).

In the calculation, only valence electrons were treated explicitly. The interaction between the valence electrons and the core electrons plus nuclei has been described using pseudopotentials. For silicon and carbon,

(18) Brookhart, M.; Green, M. L. H. *J. Organomet. Chem.* **1983**, *250*, 395–408.
(19) Cossee, P. *J. Catal.* **1964**, *3*, 80–88.
(20) Car, R.; Parrinello, M. *Phys. Rev. Lett.* **1985**, *55*, 2471–2474.
(21) Perdew, J. P.; Zunger, A. *Phys. Rev.* **1981**, *B23*, 5048–5079.

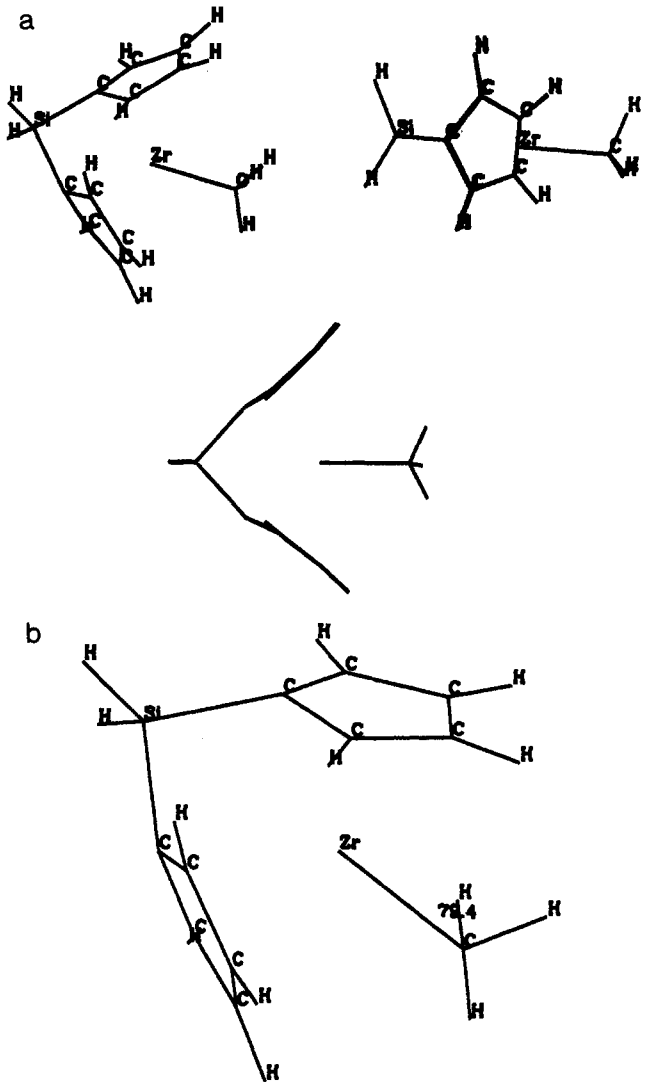

Figure 1. Structure of the energy minimized zirconocene complex $(SiH_2Cp_2)ZrCH_3^+$ studied, obtained by using the AIMD method. (a) Initial minimized structure, taken from three different points of view. (b) Structure after simulated annealing revealing an α-agostic interaction.

fully nonlocal pseudopotentials of the Bachelet–Hamann–Schluter type[22] were employed which explicitly include s and p angular components. The pseudopotential for Zr has become available through recent development in pseudopotentials, i.e., the very soft Vanderbilt pseudopotentials.[23] We performed preliminary tests on this pseudopotential and found that for an energy cutoff of 25 Ry (1 Ry ≡ 1314 kJ/mol) in the plane wave expansion of the wave functions, the total energy of a single zirconium atom has leveled off. Moreover, using this cutoff, the experimental value of the lattice parameter for ZrO_2 in its simple cubic structure was reproduced within 1%. However, in order to describe the pseudopotential for carbon accurately, an energy cutoff of 35 Ry was required. The calculation on the zirconium complex was consequently performed with an energy cutoff of 35 Ry, corresponding to a total of about 37 000 plane waves for describing the electronic state of the Zr complex.

For the purpose of visualization we made additional use of the Biosym InsightII software tools,[24] implemented on a Silicon Graphics workstation. The initial geometries were taken from ref 3. Since details of the geometry are not given in ref 3, angles and interatomic distances were taken as given in ref 3, and the other parameters were given reasonable values after visual inspection of the structures. Starting from these initial geometries, energy minimizations were performed on the free zirconocene cation, the reactant π-complex, the transition state, and the product state.

(22) Bachelet, G. B.; Hamann, D. R.; Schlüter, M. *Phys. Rev.* **1982**, *B26*, 4199–4228.
(23) Vanderbilt, D. *Phys. Rev.* **1990**, *B41*, 7892–7895.
(24) Initial structural models before being subjected to the AIMD package were developed using software programs from BIOSYM Technologies of San Diego; displayed using *Insight II*.

Table 1. Comparison of Some Geometrical Data Obtained by a Hartree–Fock Method, the Current AIMD Method, and Experimentally[a]

			present work (AIMD)	
	exptl[25,26]	Hartree–Fock[3]	**1a**	**1b**
distance Zr–C_{methyl}	2.252	2.26	2.24	2.21
distance Zr–C_{ring}	2.50	2.52	2.54	2.49
individual Zr–C_{ring} distances			2.92, 2.68	2.56, 2.56
			2.92, 2.68	2.55, 2.54
			2.46, 2.34	2.43, 2.42
			2.31, 2.27	2.44, 2.42
			2.46, 2.33	2.46, 2.45
average distance per C_p			2.61, 2.46	2.49, 2.48
ring centroid–Zr–ring centroid angle	127.5	123.5	137.5[b]	134.0[b]
Si–H distance	1.48	1.42	1.50	1.51
Si–C_{ring}	1.87	1.89	1.87	1.92

[a] Distances are given in angstroms, angles in degrees. Structures **1a** and **1b** are the structures displayed in Figure 1a and 1b, respectively. For further discussion see text. Since Si–H bond lengths can usually not be well measured with X-ray diffraction, experimental Si–H distances refer to standard literature values for such a bond. The two Si–H as well as the two Si–C_{ring} distances come out essentially identical from our simulations. [b] These values are relatively high compared to the experimental value (column 1) and the value calculated at the Hartree–Fock level (column 2). Our value has, like the Hartree–Fock result, been obtained from energy minimizations. Our molecular dynamics simulation, however, revealed an average value close to 130°.

In addition, molecular dynamics simulations were performed at a constant temperature of 400 K starting from the ethylene–zirconocene π-complex. The temperature of 400 K is within the range of experimentally employed polymerization temperatures. The simulation was carried out over a time span of 500 fs with time steps of about 0.1 fs. Temperature was kept constant within 40 K from the average value of 400 K by rescaling the velocities. The temperature as calculated from the atomic velocities was checked at time steps of 0.1 fs. No symmetry constraints of any kind were imposed during any of the calculations presented here. A typical run of 500 fs of simulation including preliminary energy minimization took some 400 h on the aforementioned IBM RISC 6000 hardware configuration.

3. Results and Discussion

3.1. Free Zirconocene Cation. We will discuss the free zirconocene cation $(SiH_2Cp_2)ZrCH_3^+$ in detail, whereas for the species following thereafter (including ethylene or the final product) we will indicate specific characteristics only. Also, because no experimental structural data are available on the species while reacting, such discussion is less useful, i.e., only theoretical results can be mutually compared.

The initially optimized structure of the zirconocene ion $(SiH_2Cp_2)ZrCH_3^+$ is depicted in Figure 1a. Some geometrical data obtained on the optimized zirconocene ion are collected in Table 1, which contains our results and Morokuma's Hartree–Fock results, as well as experimental data.[25,26] It should be noted, however, that the experimental data have been obtained on crystals, which might not show identical geometrical data as found in the gas phase or in a solvent, i.e., for isolated metallocene complexes. Also, experimental data were obtained on a series of related *neutral* Zr dichloro species. This is evident when studying experimental crystal structures, but differences between such a structure and the catalytically active cationic species might be present. Despite these possible reasons for discrepancies, both the overall AIMD optimized structure and the Hartree–Fock result of Morokuma et al. agree fairly well with the experimentally

(25) Bajgur, C. S.; Tikkanen, W. R.; Petersen, J. L. *Inorg. Chem.* **1985**, *24*, 2539–2546.
(26) Yang, X.; Stern, C. L.; Marks, T. J. *J. Am. Chem. Soc.* **1991**, *113*, 3623–3625.

determined structure. In order to understand some of the differences, it should be remembered that in ref 3 local C_{5v} symmetry on each Zr–Cp unit and C_s symmetry for the $(SiH_2Cp_2)Zr$ species were imposed, whereas in our AIMD calculations no symmetry constraints were imposed whatsoever. From the experimental compilation of Bajgur et al.,[25] comprising both bridged and unbridged dichloro metallocenes, it is corroborated that the ring-centroid–metal–ring-centroid angle Φ is relatively constant within this series of compounds, in fact, $\Phi = 127.5 \pm 5.5°$, with the value of 125.4° for the only Si-bridged zirconocene species mentioned in this compilation. Our AIMD result of 137.5° seems somewhat high here, but here we should notice that, due to the somewhat larger nonplanarity of the Cp ring as we found it from the AIMD calculations (for further discussion see below), the calculated angle is expected to be somewhat larger, for the ring-centroid positions were calculated as the center of gravity. Moreover, from the dynamics simulations to be mentioned later it was corroborated that the time-averaged value for this angle as obtained from our AIMD simulations is close to 130°, which is in much better agreement with experiment. The three values for the $Zr–C_{methyl}$ distance agree well. The symmetry imposed by Morokuma et al. resulted in five equal $Zr–C_{ring}$ distances (2.52 Å), whereas experimentally, slightly varying values have been found, as confirmed by our AIMD results.

Next, within a Cp ring we denote the carbon atom bonded to the Si by C_1, the two carbon atoms bonded to C_1 are denoted by C_2 and C_5, and the remaining two carbon atoms are named C_3 and C_4. According to the experimental data, the $C_3–C_4$ bond distance is consistently shorter by ca. 0.04 Å than the other C–C bonds in the ring (in fact, this conclusion was already drawn and presented by Bajgur et al. in their paper[25]). This effect could not be revealed from Morokuma's calculations, where symmetry conditions were imposed on the Cp rings, but the effect is clearly shown by the present AIMD results, where the $C_3–C_4$ distance is shorter than the other C–C bond lengths by ca. 0.03 Å.

The experimental structural data have revealed nonplanar Cp rings, which was revealed by both the Hartree–Fock[3] and the AIMD calculations, but only the AIMD method revealed larger $Zr–C_{ring}$ distances for C_3 and C_4, in full accordance with the experimental findings. The nonplanarity (see Figure 1a) of ca. 0.3–0.4 Å as obtained from the AIMD results overestimates the experimental result of ca. 0.06 Å displacement of the C_3 and C_4 atoms out of the $C_1–C_2–C_5$ plane.

As far as the Cp bond angles are concerned, the differences in Cp ring C–C bond lengths does not seem to be reflected to any major extent in the CCC valence angles within the ring. The AIMD calculated value ranges from 106 to 108°, in accordance with available experimental data.[25]

The Si–H distances are 1.42 Å according to Morokuma's optimized structure and 1.50 Å in our structure, whereas according to literature the standard Si–H distance is 1.48 Å.[27] The AIMD optimized value is thus slightly closer to the experimental value. The Si–C distances (Si bond to Cp) are very similar, 1.89 versus 1.87 Å from ref 3 and the present simulations, respectively.

In agreement with the Hartree–Fock results,[3] our calculations revealed a 180° angle for $Si–Zr–C_{methyl}$, although experimental structural data revealed a bent structure. However, as argued by Morokuma et al., the experimental data were obtained on a crystalline structure with the negative $CH_3B(C_6F_5)_3^-$ counterion nearby. Moreover, according to Morokuma's calculations, the bending is very soft, i.e., setting the $Si–Zr–C_{methyl}$ angle to 135° yielded an energy difference of only 2 kcal/mol as compared to the 180° situation. We have not yet checked this with the AIMD scheme employed in the present work.

As far as the positioning of the Zr with respect to the Cp rings is concerned, we already noted the unidentical Zr–Cp carbon distances. Furthermore, from the present energy minimizations (AIMD) we noticed that the Zr is not placed symmetrically between the Cp rings. This might be considered somewhat surprising. Therefore, we tried to further energy minimize the structure by a simulated annealing step. This procedure revealed a somewhat different geometry, which is displayed in Figure 1b. Some of the relevant geometrical data are given in Table 1. The nonplanarity of the Cp rings, which was ca. 0.3–0.4 Å in the former structure (Figure 1a, see the discussion above), is reduced to 0.06 Å in the structure in Figure 1b, which is in excellent agreement with the experimental value of 0.06 Å. The energy minimized structure obtained after simulated annealing has the Zr placed symmetrically between the two Cp rings, and an α-agostic interaction has appeared between one of the methyl hydrogens and the Zr atom, viz. Figure 1b. The energy difference between the structures shown in Figure 1 (parts a and b, respectively) amounts to 28 kcal/mol. For the structure shown in Figure 1a, the average force after energy minimization was 0.02 hartree/bohr, whereas for the structure of Figure 1b this was down to 0.0013 hartree/bohr. From the molecular dynamics simulations to be discussed later it was revealed, however, that the structures are very flexible at ambient temperature.

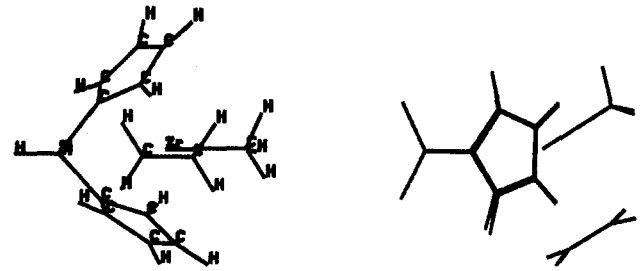

Figure 2. Structure of energy minimized reactant π-complex $(SiH_2Cp_2)ZrCH_3(C_2H_4)^+$, obtained by using the AIMD method. The figure shows an eclipsed state of ethylene and methyl as suggested by Brintzinger et al. on the basis of extended Hückel calculations,[10] although Jolly and Marynick[14] have found a staggered conformation.

3.2. Reactant π-Complex. The AIMD energy minimized structure of the π-complex $(SiH_2Cp_2)ZrCH_3(C_2H_4)^+$ is depicted in Figure 2. The structure does *not* show α-H agostic interaction, in accordance with the results published by Morokuma et al.[3] and Janiak.[11] Agreement with these less rigourous types of calculations might be fortituous, however, in particular because of the sensitivity of the final results obtained from calculations, as has been shown and emphasized by Ahlrichs et al.[16] Apparently the reaction is not primarily driven by an α-H agostic interaction. We will, however, further elaborate on this when discussing the results from the dynamics simulations.

The calculated structure revealed the occurrence of an eclipsed state of the ethylene and the methyl groups. The same result was obtained by Brintzinger et al.[10] from EHT calculations. Furthermore, the SiH_2Cp_2 system geometry remains almost unchanged as compared to the initial Zr complex without the ethylene.

3.3. Transition State. Our calculations showed essentially no barrier to reaction when going from the reactant π-complex to the product state with the propyl group formed. This is in contrast to the Hartree–Fock results reported by Morokuma et al.,[3] which revealed a barrier of 25 kJ/mol, but our result is in agreement with the data from Ahlrichs et al.,[16] albeit the latter group has studied a somewhat different species, i.e., $Cp_2TiCH_3^+H_2C{=}CH_2$ (Ti instead of Zr, and nonbridged). In this respect it needs mentioning that Morokuma et al. found the activation energy to be rather strongly dependent on the actual level of calculation; the higher level of calculation (including the MP2 level for accounting for electron correlation) yielded the lower value of 25 kJ/mol. Moreover, Ahlrichs et al. from their Hartree–Fock calculations found that the absence of a barrier of activation was first revealed when optimizing the geometry at the MP2 level or,

(27) Clark, T. *A Handbook of Computational Chemistry*; John Wiley & Sons: New York, 1985.

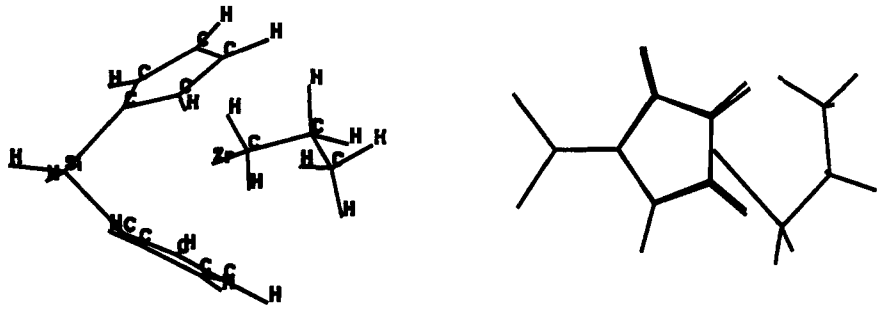

Figure 3. Structure of the energy minimized product state $(SiH_2Cp_2)ZrC_3H_7^+$ obtained using the AIMD method, taken from two different points of view.

alternatively, by using DFT. Since the AIMD method is also based on DFT, their result for the Ti complex essentially agrees with our result for the Zr complex. These data also indicate that the level of calculation as employed by Morokuma et al. was too low to obtain a reliable outcome.

Since no barrier could be found for the transition from the reactant π-complex to the product state with the propyl group formed, as will also be confirmed by the molecular dynamics results to be presented later in this paper, one might put forward the question as to whether the π-complex structure is a minimum energy structure. The structure we obtained after energy minimization had an average force on the atoms of 0.005 hartree/bohr. It is difficult to assert that this is a true local minimum. The fact that the structure did not readily transform to the product state when no barrier is present might well be a consequence of the slowness of the steepest descent minimization procedure employed.

3.4. Product State. Figure 3 shows the energy minimized product state, i.e., $(SiH_2Cp_2)ZrC_3H_7^+$. The conformation of the final product state exhibits γ-H agostic interaction (Zr–H distance 2.10 Å). As compared to the free zirconocene ion and the π-complex minimized employing the AIMD method, the Si–C_{ring} distances have clearly increased from 1.87–1.89 to 1.92–1.93 Å, in contrast to the observations reported in ref 3. With respect to the distances within the Cp rings, no appreciable changes were observed, again compared to the C–P optimized free zirconocene ion and π-complex. As expected, the distance between the Zr atom and the methyl C atom, which now makes part of the formed propyl group, has increased from about 2.24 to 2.55 Å in the product complex. The angle C_{ring}–Si–C_{ring} varied between 96° and 91°, and the angle Cp–Si–Cp (the coordinates for Cp defined as the center of gravity of the Cp ring) ranged from 79° to 86° for the series of structures comprising the two free zirconocene ions, the π-complex, and the energy minimized product state.

Finally, a few remarkable differences with the previously obtained structures, specifically those of ref 3, were observed. First, the Zr–Si distance of 3.06 Å in the free zirconocene structure and 3.21 Å in the π-complex is found to be increased to 3.39 Å in the product structure. Furthermore, a decrease of the Cp–Si–Cp opening angle was observed as compared to the π-complex and the transition state. Looking in more detail, the Cp rings in the π-complex and in the transition state are nonplanar, whereas the product state has almost planar Cp rings.

3.5. Molecular Dynamics: Chemical Reaction Dynamics. The former sections detailed the information obtained from energy minimization of the various complexes employing the AIMD method. Consequently, these could, at least in principle, be compared to equivalent simulations carried out at the Hartree–Fock level or with LDF methods, e.g, the results presented by Morokuma et al. and by Ahlrichs et al. These results all relate to static properties of the system. Applying the full potential of the AIMD method allows the molecular system to be simulated in real time, thus revealing unique information related to the dynamics of the system. It is this specific information we will

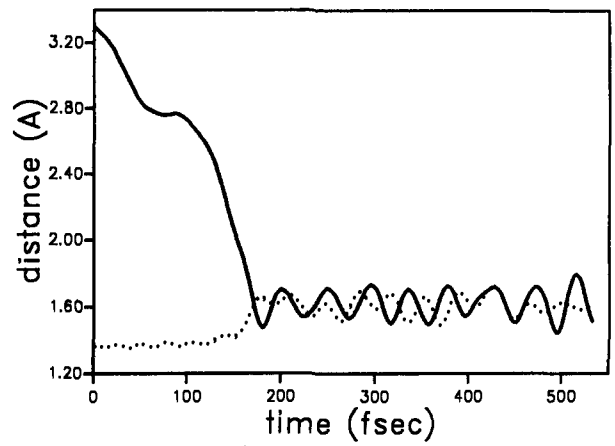

Figure 4. Time evolution of the methyl/ethyl C–C distances during the molecular dynamics simulation. The solid curve represents the distance between the methyl carbon atom and the nearest ethylene carbon atom. The broken line represents the ethylene internal C–C bond length.

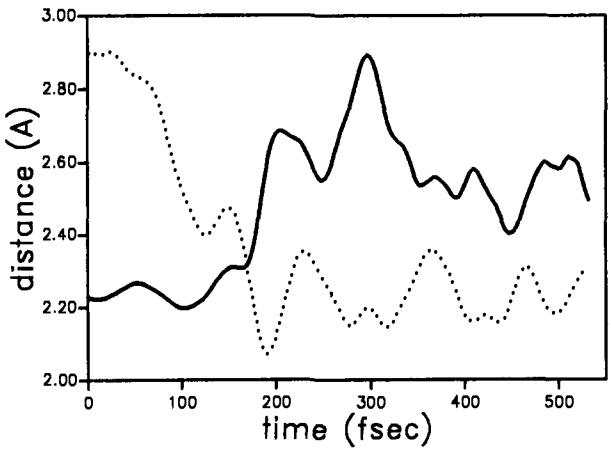

Figure 5. Time evolution of the Zr–C distance for the methyl carbon atom (solid curve) and for one of the ethylene carbon atoms (dotted curve).

discuss in the present section. For this purpose, the dynamics of the $(SiH_2Cp_2)ZrCH_3^+H_2C{=}CH_2$ π-complex was simulated at a constant temperature of 400 K. We started the molecular dynamics simulations from the less stable structure (without α-agostic interaction, Figure 1a), which might provide extra information with respect to the necessity of α-agostic interaction for the ethylene insertion to proceed.

As a result of the dynamics simulations, Figures 4–8 display geometrical variables as a function of simulation time. Figure 4 displays the carbon–carbon distances within the set of three carbons that are supposed to form the propyl group in the course of the reaction. From Figure 4 it is quite apparent that the reaction between the methyl and the inserting ethylene unit takes placein the time span ranging from approximately 70 to 170 fs. Thereafter, the C–C distances still vary within the normal limits

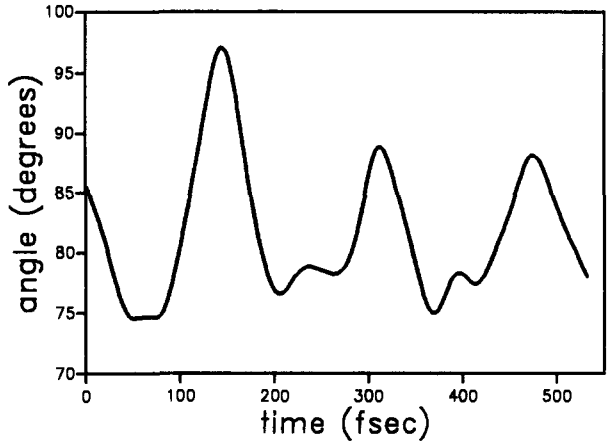

Figure 6. Time evolution of the Cp–Si–Cp angle. For the Cp coordinates, the center of gravity of the ring was taken.

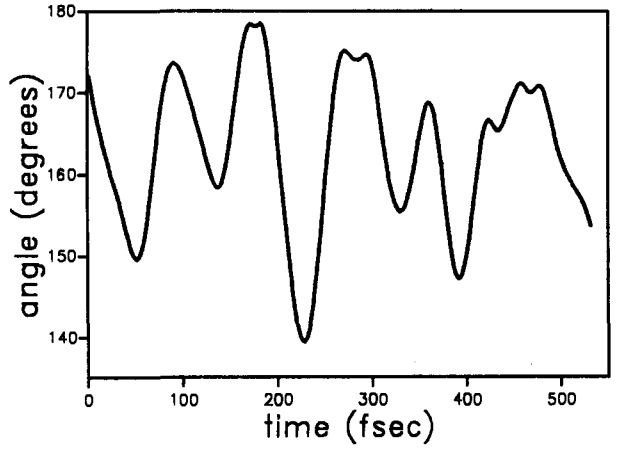

Figure 7. Time evolution of the Si–C–Cp angle, where the coordinate taken for the Cp ring is the center of gravity of the ring, which implies that for a nonplanar ring system it lies somewhat outside what one would define as the ring plane.

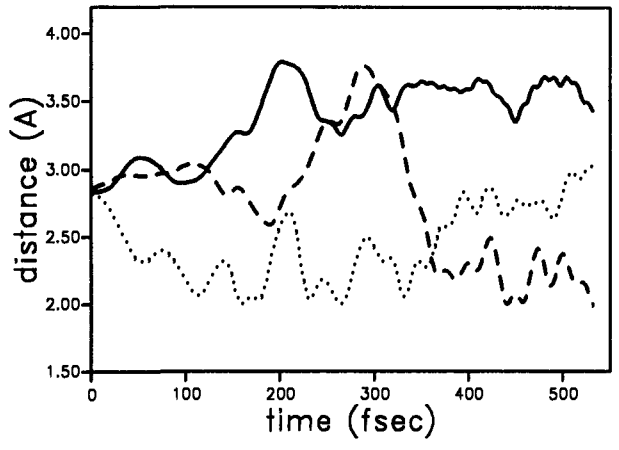

Figure 8. Time evolution of the distance between the Zr atom and each of the three hydrogen atoms belonging to the methyl group (the original methyl group bonded to the Zr). The time evolution of one of the hydrogen atoms depicted by the dotted curve shows the development of α-H agostic interaction. Later on in the simulation (after about 450 fs), one of the other protons (broken curve) exhibits γ-H agostic interaction.

characteristic of C–C vibrations. So, completely unexpectedly and surprisingly, the simulation was successful in the sense that the ethylene reacted with the methyl group to form a propyl group within a time span of about *100 fs*. We believe that this is unexpectedly fast, notwithstanding the fact that we had already reached the conclusion that no reaction barrier was involved on the basis of the static energy minimizations.

With respect to the importance of explicitly following the dynamics of the system, we notice that the time span of 100–150 fs corresponds to a frequency of 300 cm^{-1}. This implies that the molecular motions at this time scale or slower cannot relax during the time in which the reaction takes place, i.e., not all geometrical variables in the molecule are able to relax such that the minimum energy structure is reached. Such slow motions do exist in the species under investigation, however. As a consequence, trying to obtain similar information from static energy minimization of the various intermediate states, in particular the transition state, might not even be realistic.

Now that we have determined the time span in the simulation during which the reaction actually takes place, we may analyze other variables as a function of simulation time and inspect whether any of these variables have an apparent relation to the actual chemical reaction. First, Figure 5, displaying the Zr–C distances for both the methyl carbon and one of the ethylene carbons, shows the interchange between these two carbons with regard to which one is closest to the Zr ion. This possibly implies that with each subsequent monomer insertion the active site isomerizes, i.e., a chain migratory insertion mechanism is involved. Figure 6 shows the time evolution of the Cp–Si–Cp angle. On the basis of the present simulation, there does not seem to be any obvious relation with the insertion reaction. Furthermore, the present simulations demonstrate that the Cp rings fluctuate heavily around the Zr ion. Although Figure 6 does display some of the relevant information, this is evidently not *all* the relevant information, because additional information on, e.g., the Cp–Zr–Cp variable, is required for a more detailed picture of the overall flexibility of the molecular system.

Another geometrical variable that relates to the flexibility of the system, indirectly also related to the flexibility of the Cp rings with respect to the bonding to the Zr ion, the time evolution of the Si–C–Cp(center ring) angle plotted in Figure 7 displays substantial variation, although no obvious correlation with the reaction path was observed. This was corroborated from the fact that the fluctuations observed seem constant during the entire simulation period, both before and after the insertion reaction and the formation of the propyl group. Figure 8 displays the time evolution of the distance between the Zr atom and each of the three hydrogen atoms belonging to the methyl group (the original methyl group bonded to the Zr), which relates to a possible α-H agostic interaction necessary for the reaction to take place. This plot (dotted curve) shows the development of an α-H agostic interaction during the reaction. However, we recall that the molecular dynamics simulation was started from a geometry without an α-agostic interaction in the energy-minimized π-complex. Thus, for the moment, the presence of an α-H agostic interaction does not seem to be a prerequisite for the reaction to take place, although it forms *during* reaction. Further investigations on this item are in progress.

From the dynamics simulations it was revealed that the ethylene is inserted in a *cis* manner, in accordance to what is generally accepted, and a γ-H agostic interaction is present in the product state, although the time evolution of the relevant Zr–H distances as displayed in Figure 8 showed that this interaction is subject to a dynamic process, i.e., the methyl protons exchange their positions so that they alternate being involved in the γ-H agostic interaction. The actual relevance and importance of this γ-H agostic interaction are therefore not obvious.

Finally, with respect to the discussion on the time evolution of geometrical parameters, from the analysis of "geometrical parameter" versus "simulation time" plots presented above, cf. Figures 4–8, it is concluded that no particular geometry change seems required for the reactant species in order to have the reaction proceed. The starting geometry was apparently sufficient to let the reaction proceed. It is only *during* the reaction that the values of some of the geometrical parameters are really changing.

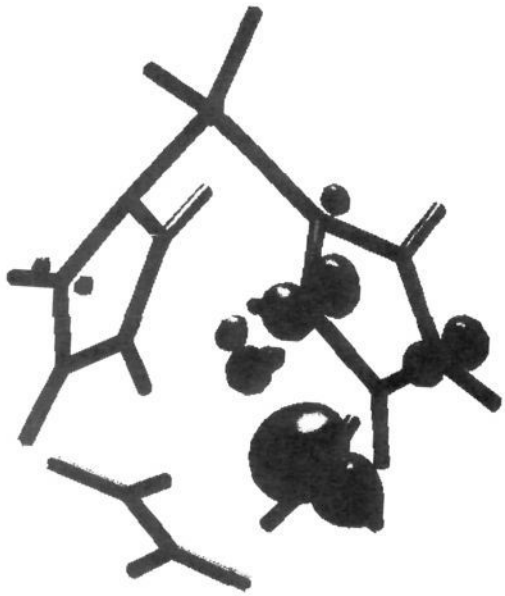

Figure 9. Electron distribution of the HOMO in the reactant π-complex, e.g., as depicted in Figure 2, which is found primarily centered at the zirconium-bonded methyl group.

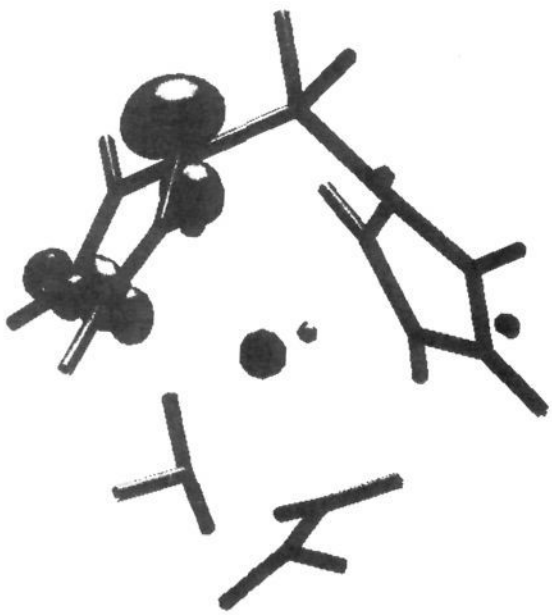

Figure 10. Electron distribution of the HOMO during the reaction, e.g., at $t \approx 170$ fs, which is seen to be located at one of the Cp rings.

So far we have mainly discussed the geometrical parameters as a function of the simulation time. When considering the chemical reaction process and the mechanism involved, apart from an interest in the necessary bond breaking and bond formation involved in the chemical reaction, basically any change in geometrical parameters must be a consequence of energetical changes rather than the reverse. Therefore, geometrical changes in themselves do not mean anything, and we have to further analyze the energetics in order to further elaborate on the reaction mechanism. One way to analyze this is to inspect the HOMO and the LUMO of the complex along the reaction path. Figures 9–11 show the electron density distribution of the HOMO for the π-complex, the (quasi)transition state, and the product state, respectively. The HOMO in the π-complex appears to be primarily centered at the zirconium–bonded methyl group. Then,as can be corroborated from Figure 10, during the reaction (range near transition state) the HOMO is located at one of the Cp rings, and in the final product state it becomes located at the

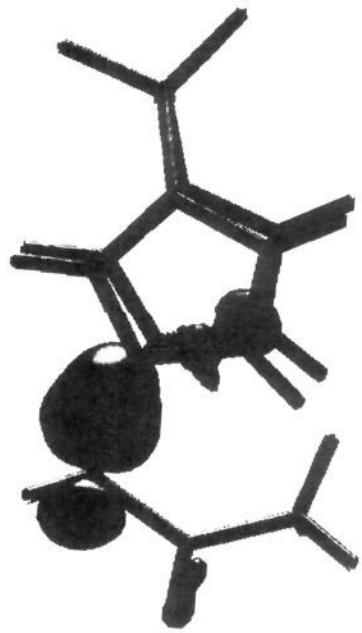

Figure 11. Electron distribution of the HOMO in the final product state, where it is located at the propyl α-carbon atom.

propyl α-carbon atom (Figure 11). These observations, in particular the specific location of the HOMO at one of the Cp rings during the reaction, are possibly intimately related to the fact that Cp rings have thus far been (experimentally) required for exhibiting good catalytic performance.

4. Final Discussion and Conclusions

The structure of the metallocene cation energy minimized with the AIMD method agrees well with the experimentally obtained crystal structures of related complexes. Typical features of the structure, like differences in distances between the mutual C atoms within a Cp ring, as well as differences in distances between the C atoms of the Cp ring and the Zr atom, were revealed. The static energy minimizations suggested that the insertion reaction of ethylene with the methyl group of the zirconocene complex to form propyl occurs without an activation barrier.

From the full ab initio molecular dynamics simulation, the insertion of π-coordinated ethylene into the Zr–C bond leading to propyl formation was revealed. This reaction took place in a time span of the order of 150 fs, which is unexpectedly fast. Starting from the π-complex, the ethylene shifts toward the methyl group that represents the polymer chain. This results in a four–center transition state, loosely described as a metallocyclobutane ring-type complex. At the aforementioned time scale of the reaction, however, it might be questioned whether it still makes sense to talk, referring to the previously proposed reaction mechanism, in terms of a four-center transition state, one of the primary details of the Cossee mechanism. The time scale of the reaction is so short that it does not seem useful to adopt terminology related to the kind of quasiequilibrium structures involved in some traditionally proposed schemes. In this respect, we recall that we have not found a true (quasistable) transition state. The same applies to the observation of a possible relevance of α-H agostic interaction, referring to the Brookhart and Green mechanism.

In the transition state, the ethylene and the methyl appear to be in an eclipsed state. Whereas we started the molecular dynamics simulations from an energetically less favorable geometry which did not have an α-agostic interaction, during the molecular dynamics run, an α-H agostic interaction is established in the early stages of the insertion process. The final complex seems stabilized by γ-H agostic interaction, although severely influenced by the dynamics and not by β-H agostic interactions.

From the dynamics simulations it was found that the Cp rings are very flexible. Furthermore, during the reaction the HOMO is transferred from the initial Zr–C bond, via *one* of the Cp rings during what we might call a transition-state region, to the novel Zr-C bond in the final product.

We feel it important to emphasize that the present result is not at variance with an experimentally observed temperature dependence of the reaction rate. The latter implies an energy barrier. In this context our results only indicate that this barrier is not related to the insertion step, and consequently the energy barrier to polymerization must be ascribed to another step in the overall polymerization scheme.

The results presented in this paper demonstrate that it has become feasible to study the full dynamics of a real catalytic reaction, from the reactant complex to the product state, whereas until now such processes could be studied only by static energy minimizations revealing a typical quantity such as the activation energy. From this type of theoretical modeling, previously inaccessible insight into the polymerization reaction can be obtained, and as such it is a new, powerful tool for further investigating and elucidating fast chemical reaction mechanisms.

Acknowledgment. Albeit we started our simulations with geometries approximate to those published in ref 3, the authors gratefully acknowledge Prof. Morokuma and Dr. Kuribayashi for providing us with their actual calculated minimum energy structures (Cartesian coordinates), which obviously helped us to compare and further interpret the various data sets. We also gratefully acknowledge Prof. Reinhart Ahlrichs and Dr. Horst Weiss for making available a preprint of their work. Dr. Kari Laasonen is acknowledged for his cooperation in construction of the Vanderbilt pseudopotential for zirconium. Dr. Michele Parrinello and Dr. Stefano Patarnello are acknowledged for very useful and stimulating discussions. The management of DSM Research is thanked for their permission to publish this work.

Supplementary Material Available: Cartesian coordinate files of the structures as revealed from the static energy minimizations (2 pages). This material is contained in many libraries on microfiche, immediately follows this article in the microfilm version of the journal, and can be ordered from the ACS; see any current masthead page for ordering information.